

# Single-Crystalline ZnO Microtubes Formed by Coalescence of ZnO Nanowires Using a Simple Metal-Vapor Deposition Method

Jong Seok Jeong,<sup>†</sup> Jeong Yong Lee,<sup>\*,†</sup> Jung Hee Cho,<sup>‡</sup> Han Jong Suh,<sup>‡</sup> and Cheol Jin Lee<sup>\*,‡</sup>

Department of Materials Science and Engineering, Korea Advanced Institute of Science and Technology,  
373-1 Guseong-dong, Yuseong-gu, Daejeon 305-701, Republic of Korea, and  
Department of Nanotechnology, Hanyang University, 17 Haengdang-dong, Seongdong-gu,  
Seoul 133-791, Republic of Korea

Received April 15, 2004. Revised Manuscript Received March 3, 2005

Single-crystalline ZnO microtubes were synthesized by a simple metal-vapor deposition method. The ZnO microtubes, which had outer diameters in the range of 0.3–2  $\mu\text{m}$  and wall thickness in the range of 100–500 nm, indicated a faceted hexagonal shape. In addition, it was found that there were many incomplete ZnO microtubes, which indicate the morphology assembled with several nanowires at the tip part of the microtubes and prismatic tubular morphology at the bottom part of the microtubes. It is suggested that the ZnO microtubes were formed by the coalescence of ZnO nanowires due to a high reaction temperature of 950  $^{\circ}\text{C}$  and optimized oxygen supplement when ZnO nanowires were grown on a large ZnO grain. We discuss the growth mechanism of the ZnO microtubes in detail.

## Introduction

The control of the shape and the orientation of oxide nano-/microcrystallites with various morphologies such as wire, rod, belt, and tube have attracted much attention because of their great potential for fundamental studies of the effects of morphology, dimensionality, and size on their physical and chemical properties as well as for their application in optoelectronic devices.<sup>1,2</sup> Recently, zinc oxide (ZnO) nano-/microcrystallites with various morphologies have been synthesized by many researchers using various methods.<sup>3–7</sup> ZnO, which has a direct band gap of 3.37 eV and large exciton binding energy of 60 meV, can realize practical applications in the area of nanoscale laser diodes, sensors, varistors, and so on. Especially, the tubular structures of nano-/microcrystalline materials become important because a high porosity and a large surface area are required to fulfill the demand of high efficiency and activity in numerous applications. For instance, the development of new functional materials with high porosity is required for better and

optimized performances of dye-sensitized photovoltaic cells, dimensionally stable anodes (DSA), metal-ion batteries, electrochemical supercapacitors, hydrogen storage devices, biosensors, and gas sensors.<sup>8</sup> Tubular structures of several binary oxide systems, including  $\text{TiO}_2$ ,<sup>9,10</sup>  $\text{SiO}_2$ ,<sup>11</sup>  $\text{Ga}_2\text{O}_3$ ,<sup>12</sup>  $\text{In}_2\text{O}_3$ ,<sup>13</sup>  $\text{VO}_x$ ,<sup>10</sup> and  $\text{Y}_2\text{O}_3$ ,<sup>14</sup> have been synthesized by various methods, and several researchers have synthesized ZnO nano-/microtubular structures using several methods, such as template, chemical reaction, pyrolysis, thermal treatment, and so on.<sup>15–20</sup> Up to now, some research groups demonstrated the synthesis of tubelike ZnO arrays at low reaction temperature below 100  $^{\circ}\text{C}$  using a chemical solution route,<sup>8,21</sup> which has advantages that simple procedures, no sophisticated equipment, and low reaction temperature are needed. However, the entire reaction time of these techniques is as long as 2 days<sup>8</sup> while thermal vapor methods generally need a reaction time below 1 h. Despite much progress in the

\* To whom correspondence should be addressed. E-mail: j.y.lee@kaist.ac.kr (J.Y.L.); cjlee@hanyang.ac.kr (C.J.L.). Tel: +82-42-869-4216 (J.Y.L.). Fax: +82-42-869-4276 (J.Y.L.).

<sup>†</sup> Korea Advanced Institute of Science and Technology. E-mail: J.S.Jeong@kaist.ac.kr (J.S.J.).

<sup>‡</sup> Hanyang University. E-mail: hizey@nate.com (J.H.C.); zikze10@hanmail.net (H.J.S.).

- (1) Hu, J. T.; Odom, T. W.; Lieber, C. M. *Acc. Chem. Res.* **1999**, *32*, 435.
- (2) (a) Wang, Z. L.; Kang, Z. C. *Functional and Smart Materials-Structural Evolution and Structure Analysis*; Plenum Press: New York, 1998. (b) Adachi, G. Y.; Imanaka, N. *Chem. Rev.* **1998**, *98*, 1479.
- (3) Lao, J. Y.; Huang, J. Y.; Wang, D. Z.; Ren, Z. F. *Nano Lett.* **2003**, *3*, 235.
- (4) Hu, P.; Liu, Y. Q.; Wang, X. B.; Fu, L.; Zhu, D. B. *Chem. Commun.* **2003**, 1304.
- (5) Park, W. I.; Yi, G.-C. *Adv. Mater.* **2004**, *16*, 87.
- (6) Kong, X. Y.; Ding, Y.; Yang, R.; Wang, Z. L. *Science* **2004**, *303*, 1348.
- (7) Park, J.-H.; Choi, H.-J.; Choi, Y.-J.; Sohn, S.-H.; Park, J.-G. *J. Mater. Chem.* **2004**, *14*, 35.

- (8) Vayssieres, L.; Keis, K.; Hagfeldt, A.; Lindquist, S.-E. *Chem. Mater.* **2001**, *13*, 4395.
- (9) Lakshmi, B. B.; Patrisi, C. J.; Martin, C. R. *Chem. Mater.* **1997**, *9*, 2544.
- (10) Rao, C. N. R.; Nath, M. *Dalton Trans.* **2003**, 1.
- (11) Hu, J.-Q.; Meng, X.-M.; Jiang, Y.; Lee, C.-S.; Lee, S.-T. *Adv. Mater.* **2003**, *15*, 70.
- (12) Graham, U. M.; Sharma, S.; Sunkara, M. K.; Davis, B. H. *Adv. Funct. Mater.* **2003**, *13*, 576.
- (13) Li, Y. B.; Bando, Y.; Golberg, D. *Adv. Mater.* **2003**, *15*, 581.
- (14) Wang, X.; Sun, X. M.; Yu, D. P.; Zou, B. S.; Li, Y. D. *Adv. Mater.* **2003**, *15*, 1442.
- (15) Xing, Y. J.; Xi, Z. H.; Zhang, X. D.; Song, J. H.; Wang, R. M.; Xu, J.; Xue, Z. Q.; Yu, D. P. *Solid State Commun.* **2004**, *129*, 671.
- (16) Gundiah, G.; Mukhopadhyay, S.; Tumkurkar, U. G.; Govindaraj, A.; Maitra, U.; Rao, C. N. R. *J. Mater. Chem.* **2003**, *13*, 2118.
- (17) Zhang, J.; Sun, L. D.; Liao, C. S.; Yan, C. H. *Chem. Commun.* **2002**, 262.
- (18) Zhang, X.-H.; Xie, S.-Y.; Jiang, Z.-Y.; Zhang, X.; Tian, Z.-Q.; Xie, Z.-X.; Huang, R.-B.; Zheng, L.-S. *J. Phys. Chem. B* **2003**, *107*, 10114.
- (19) Hu, J. Q.; Bando, Y. *Appl. Phys. Lett.* **2003**, *82*, 1401.
- (20) Hu, J. Q.; Li, Q.; Meng, X. M.; Lee, C. S.; Lee, S. T. *Chem. Mater.* **2003**, *15*, 305.
- (21) Wang, Z.; Qian, X. F.; Yin, J.; Zhu, Z. K. *Langmuir* **2004**, *20*, 3441.

synthesis of ZnO nano-/microtubes, there was no report on the synthesis of ZnO microtubes using a metal-vapor deposition method until now. Moreover, an explanation about the growth mechanism of ZnO microtubes is still desired to understand the synthesis of ZnO microtubes. Our group has studied the synthesis and the growth mechanism of ZnO nanowires using a metal-vapor deposition method.<sup>22,23</sup> As a result, we could elucidate the refined growth mechanism of ZnO nanowires.<sup>24</sup>

Here, we demonstrate that single-crystalline ZnO microtubes can be fabricated by control of oxygen gas and reaction temperature using a simple metal-vapor deposition method. Our result indicates that ZnO tubular structures are formed by a coalescence of ZnO nanowires grown on large individual ZnO grains on Al<sub>2</sub>O<sub>3</sub> substrate. We discuss the possible growth mechanism of the ZnO microtubes produced by a simple metal-vapor deposition method.

### Experimental Section

The ZnO microtubes were fabricated by a following procedure. A nickel nitrate/ethanol solution (0.01 M) was dropped onto an Al<sub>2</sub>O<sub>3</sub> substrate. After drying of the Al<sub>2</sub>O<sub>3</sub> substrate at 400 °C in ambient air, NiO particles were evenly formed on the Al<sub>2</sub>O<sub>3</sub> substrate. The substrate was loaded on a quartz boat filled with metal zinc powder (99.998%, Sigma-Aldrich) and ZnO powder (99.998%, Sigma-Aldrich). The quartz boat was inserted into a quartz tube under a constant flow of argon (flow rate: 500 sccm). After evacuation during 20 min, the quartz tube was heated to 950 °C under a constant flow of argon (flow rate: 500 sccm). The ZnO microtubes were synthesized at 950 °C for 60 min under argon flow of 500 sccm and oxygen flow of 5 sccm. After reaction, the quartz tube was spontaneously cooled to room temperature. The produced ZnO microtubes were characterized by scanning electron microscopy (SEM; Hitachi S-4700) equipped with energy dispersive spectrometry (EDS), X-ray diffraction (XRD; Rigaku KMAX PSCC MDG 2000), and transmission electron microscopy (TEM; JEOL JEM3010).

### Results and Discussion

Figure 1 shows XRD pattern and EDS spectrum of the ZnO products grown on the Al<sub>2</sub>O<sub>3</sub> substrate. The XRD reveals that the products are well-known hexagonal wurtzite ZnO as shown in Figure 1a. There is no evidence of bulk remnant materials and impurity. Generally, the relative intensity for the 0002 line of tubular structure has small intensity due to absence of the (000*n*) planes in the hollow structure. However, in this work, the intensity of the 0002 peak of the ZnO microtubes indicates high intensity. We consider that the (000*n*) planes are actually not absent because the ZnO microtubes have a large wall thickness in the range of 100–500 nm and the ZnO layer is formed on the substrate before the growth of the ZnO microtubes according to the growth mechanism of the ZnO microtubes which will be proposed later. The EDS analysis demonstrates

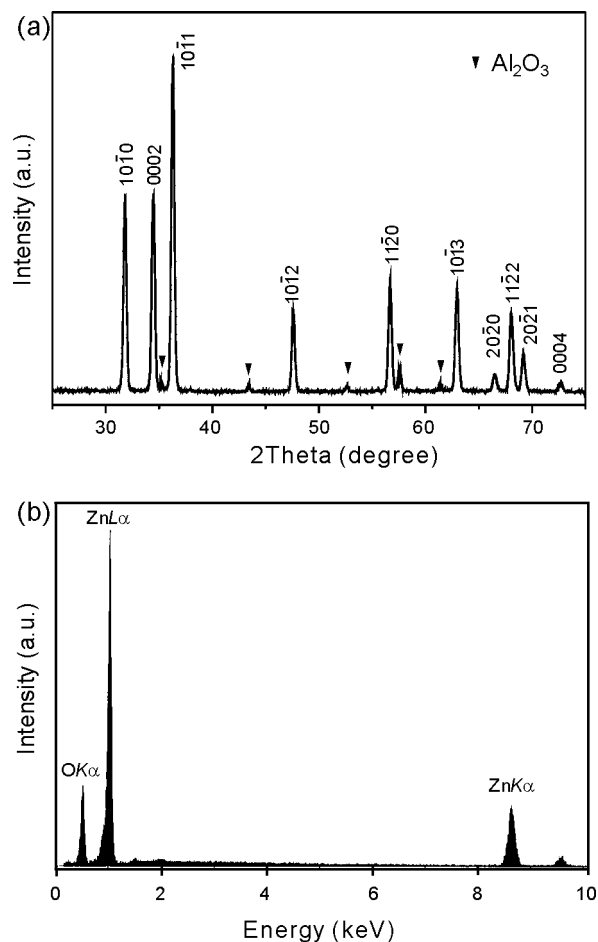


**Figure 1.** (a) XRD pattern and (b) EDS spectrum of the ZnO products produced on the Al<sub>2</sub>O<sub>3</sub> substrate.

that the products consist of only zinc and oxygen elements as shown in Figure 1b.

Typical SEM images of the synthesized products are shown in Figure 2. The SEM images reveal that the ZnO crystals with tubular shape are synthesized on the Al<sub>2</sub>O<sub>3</sub> substrate. The ZnO tubular structures have outer diameters in the range of 0.3–2 μm, wall thickness in the range of 100–500 nm, and lengths about 10 μm. The detailed geometrical morphologies are shown in Figure 2c,d. The magnified SEM images show that most ZnO microtubes have a hollow cavity and a faceted hexagonal shape. In addition, from more SEM observations, we found that there were many incomplete ZnO microtubes, which showed the special morphology assembled with several nanowires (see Figure 4). The detail growth mechanism of the microtubes will be discussed in a later section.

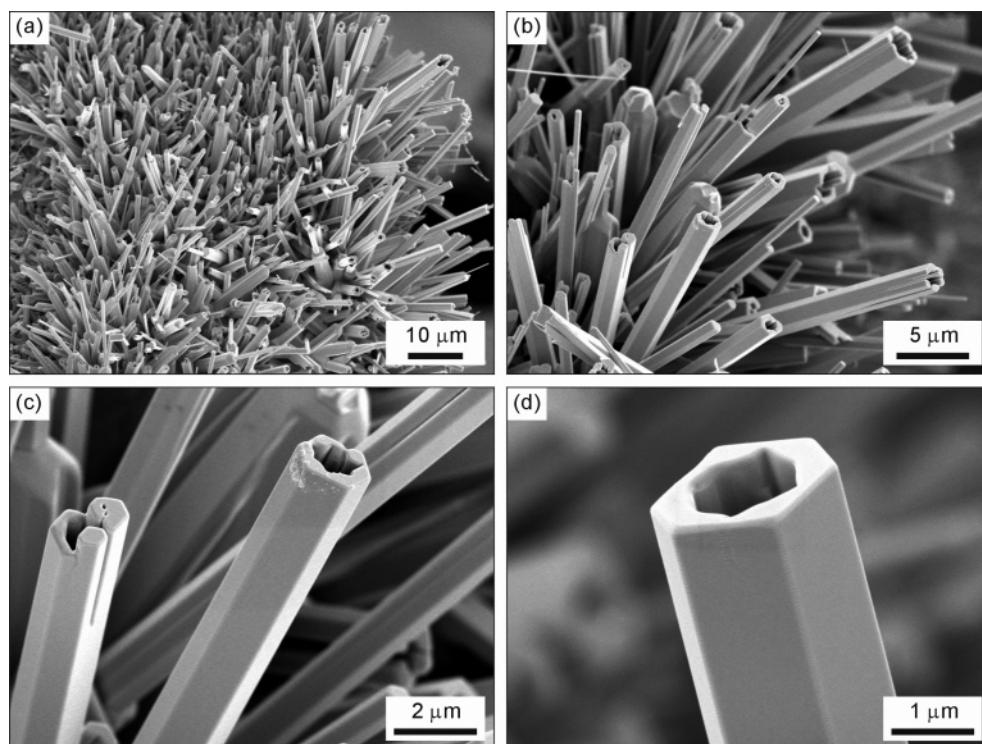
TEM analysis shows that the ZnO microtubes grow along [0001] direction and have a single-crystalline structure as shown in Figure 3. The image contrast shows that the ZnO products have a hollow cavity indicating tubular structure. We tried to investigate high-resolution TEM (HRTEM) image of the ZnO microtubes, but we had no success in getting a lattice image because the tube wall was too thick to obtain HRTEM images.

Figure 4 shows the SEM images of the above-mentioned incomplete ZnO microtubes. The side-viewed SEM images of the various morphologies of tips of the incomplete

(22) Lee, C. J.; Lee, T. J.; Lyu, S. C.; Zhang, Y.; Ruh, H.; Lee, H. J. *Appl. Phys. Lett.* **2002**, *81*, 3648.

(23) Lyu, S. C.; Zhang, Y.; Ruh, H.; Lee, H.-J.; Shim, H.-W.; Suh, E.-K.; Lee, C. J. *Chem. Phys. Lett.* **2002**, *363*, 134.

(24) Lyu, S. C.; Zhang, Y.; Lee, C. J.; Ruh, H.; Lee, H. J. *Chem. Mater.* **2003**, *15*, 3294.



**Figure 2.** Typical SEM images of the synthesized ZnO microtubes: (a, b) low-magnification SEM images of the microtubes; (c, d) high-magnification SEM images revealing geometrical morphology of the microtubes with a faceted hexagonal shape.

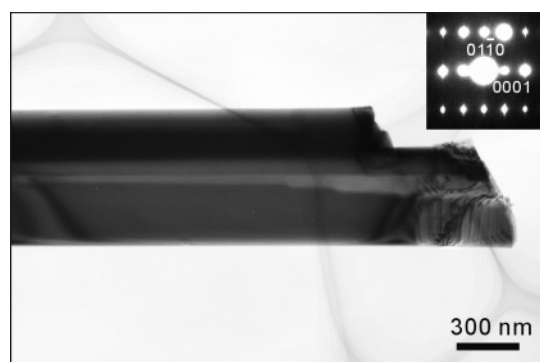


**Figure 3.** Typical TEM image and selected-area electron diffraction pattern of the ZnO microtube.

microtubes are shown in Figure 4a–d, and the top-viewed SEM image is also shown in Figure 4e. The SEM images certainly indicate that the incomplete microtubes exhibit that neighboring individual nanowires are assembled together, resulting in a hexagonal shape as shown in a dotted line indicated in the SEM images. It is likely that the incomplete ZnO microtubes show proceeding stages of their growth. Therefore, at the final growth stage, these incomplete microtubes may also have hexagonal prismatic tubular morphologies as shown in Figure 2d. From SEM observations of ZnO microtubes, we suggest that the ZnO microtubes are formed by the coalescence of neighboring nanowires grown on a large individual ZnO grain on the  $\text{Al}_2\text{O}_3$  substrate. In this work, we can find that no catalyst particle was observed at the tip of the microtubes in the SEM images and the EDS analysis also indicated that there was no evidence of the catalyst particle at the tip of the microtubes. It reveals that the catalyst particles may exist at the bottom of the microtubes. It is well-known that transition metal

oxides, such as nickel and iron monoxides (NiO and FeO), also have a catalyst effect on the growth of semiconductor nanomaterials that is similar to the metal catalyst.<sup>25</sup> In this work, we consider that the NiO catalyst just affects formation of ZnO layer on the  $\text{Al}_2\text{O}_3$  substrate and not growth of the ZnO microtubes as proposed in previous work on the growth mechanism of ZnO nanowires.<sup>24</sup> When we investigated the surface of the  $\text{Al}_2\text{O}_3$  substrate, we could find that several tens of nanometer-sized NiO catalyst particles were produced on the  $\text{Al}_2\text{O}_3$  substrate by adopting a simple baking process at 400 °C in air ambient as shown in Figure 5. The SEM image shows that the surface of the  $\text{Al}_2\text{O}_3$  substrate reveals isolated grain morphology because the  $\text{Al}_2\text{O}_3$  substrate used has a bulk crystal structure.

The proposed growth mechanism of the ZnO microtubes is shown in Figure 6. At the initial stage of ZnO microtube growth, an island of a thin ZnO layer is grown on the NiO catalyst particle. With further progression in the growth of ZnO, the thin ZnO layer gradually grows on the NiO catalyst particle and finally perfectly covers the NiO catalyst particle as shown in Figure 6a. The nucleation can occur at any of the sites on the ZnO layer. We had proposed a similar growth mechanism on ZnO nanowires in our previous work, in which the ZnO nanowires were directly synthesized not on the NiO nanoparticles but on the laterally grown thin ZnO layer originated from the NiO nanoparticles on the  $\text{Al}_2\text{O}_3$  substrate.<sup>24</sup> However, in this work, we supplied oxygen gas into the reactor during the ZnO growth and synthesized ZnO materials at a high reaction temperature of 950 °C, distinctively from our previous results.<sup>22,24</sup> As a result, the grown ZnO layers consist of large grains. In fact, it is well-known

(25) Chen, X. L.; Li, J.; Lao, Y.; Lan, Y.; Li, H.; He, M.; Wang, C.; Zhang, Z.; Oiao, Z. *Adv. Mater.* **2000**, *12*, 1432.



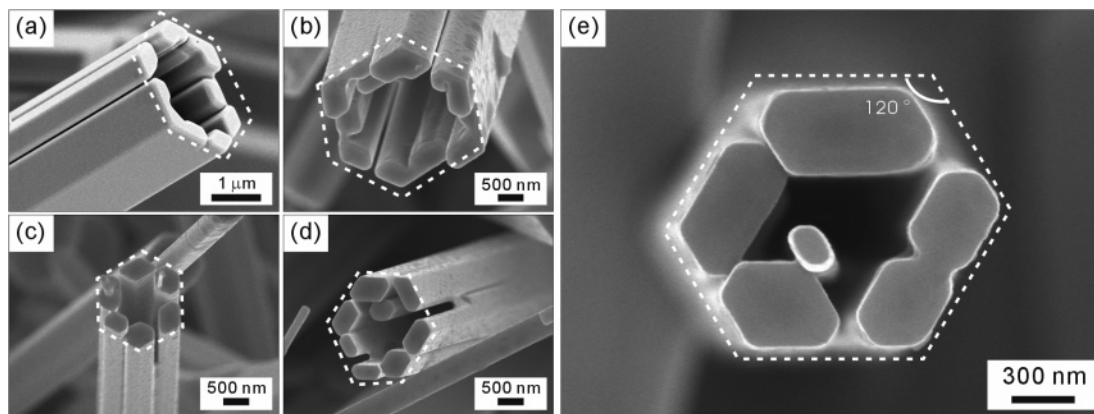


**Figure 4.** SEM images of the ZnO microtubes with the morphology assembled with several nanowires: (a–d) side-view SEM images of the tips of the incomplete microtubes; (e) top-view SEM image of the tip of the incomplete microtube.

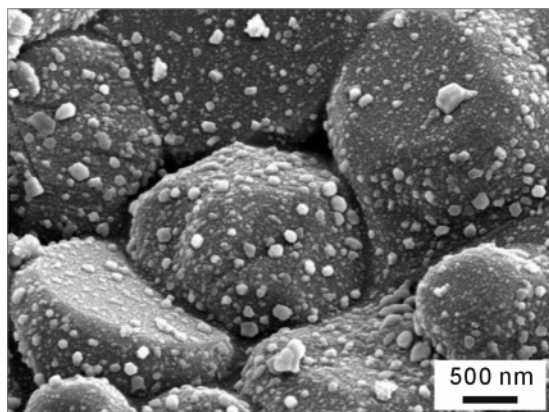


**Figure 5.** SEM image of several tens of nanometer-sized NiO catalyst particles produced on the  $\text{Al}_2\text{O}_3$  substrate.

that the grain size increases as growth temperature increases.<sup>26</sup> In the case of large grain size, several nucleation sites can be generated on one ZnO grain as shown in Figure 6b. The ZnO nuclei may selectively grow along the crystallographic orientation of the ZnO grain due to the strong epitaxial relation between the ZnO nuclei and the ZnO grain as shown in Figure 6b, resulting that the ZnO nanowires have the same direction of *c*-plane to the ZnO grain. Continuous feeding of evaporated Zn sources and oxygen elements into favorable nucleation sites will lead to vertical directional growth of the ZnO nanowires as shown Figure 6c. Therefore, the epitaxially grown nanowires within the same grain region may have the same crystallographic direction. As the growth time increases, the ZnO nanowires may grow laterally even though the lateral growth rate is much lower than that of the vertical direction as shown in Figure 6d. Moreover, a high reaction temperature may accelerate the lateral growth of the ZnO nanowires. Therefore, neighboring ZnO nanowires at the same grain region easily coalesce together as shown in Figure 6e, resulting in the incomplete ZnO microtubes as shown in Figure 4. As the reaction time increase, the complete prismatic ZnO microtubes are finally formed by the coalescence of ZnO nanowires as shown in Figure 6f. Consequently, the coalescence of ZnO nanowires contributes to the ZnO microtubular structures with single-

crystalline structure as shown in TEM results and the ZnO microtubes formed by coalescence of nanowires have a hexagonal prismatic morphology as shown in Figure 2d. This is quite different from the previous report which indicated the growth mechanism of tubelike ZnO arrays produced by chemical solution route.<sup>21</sup> While Wang et al. suggested that ZnO nanowires were formed at first on the substrates and self-adjusted in a hexagonal circle before growing into a tubular structure, we suggest that the ZnO microtubes were generated by a high reaction temperature and reasonable oxygen supplement in our work.

We have conducted additional experiments to support our suggestion that the reaction temperature and the oxygen gas play an important role in the formation of microtubes. According to our experimental results, we could not succeed in obtaining ZnO microtubes at lower growth temperature. When we increased the flow of oxygen gas from 5 to 50 sccm with argon flow of 500 sccm, neither nanowires nor microtubes were formed as shown in Figure 7a. On the other hand, when the flow of oxygen gas was reduced to 2 sccm, we can obtain just nonuniform ZnO flakes with relatively large width due to high reaction rate of ZnO crystal as shown in Figure 7b. The respective detailed morphologies are shown in the inset of Figure 7a,b to identify their structures. Our previous results also showed that only nanowires could grow when the oxygen gas was not supplied into the reactor and the reaction temperature was low.<sup>22,23</sup> These results demonstrate that the optimized reaction temperature and oxygen element are very important to synthesize the ZnO microtubes.

In this work, the synthesized ZnO microtubes have a larger diameter than that of previously reported tubular structures because the ZnO microtubes were formed by the coalescence of the ZnO nanowires. Moreover, the synthesized microtubes have a faceted hexagonal shape. To explain why the ZnO microtubes formed by coalescence of nanowires finally have a hexagonal shape morphology, it is necessary to understand thermodynamic stability of ZnO structure. Generally, the crystal exhibits a different growth behavior depending on the relative growth rates at various crystal facets. ZnO forms a polar crystal with space group of  $P6_3mc$  and *c*-axis as polar axis. In the ZnO structure, each  $\text{Zn}^{2+}$  ion is surrounded by four  $\text{O}^{2-}$  ions and vice versa. The growth velocities of the ZnO crystal in different directions are reported to be  $[0001] > [01\bar{1}1] > [01\bar{1}0] > [01\bar{1}1] > [000\bar{1}]$  under hydrothermal

(26) Meng, L. J.; Andritschky, M.; Dossantos, M. P. *Vacuum* **1994**, *45*, 19.

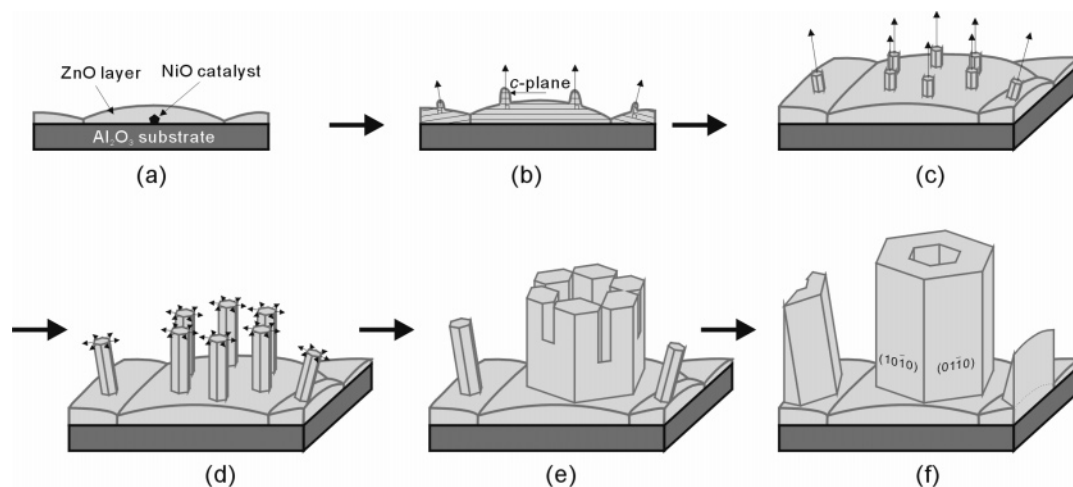


**Figure 6.** Schematic diagram of the proposed growth mechanism of the ZnO microtubes formed by coalescence of the ZnO nanowires: (a) thin ZnO layer formed on the NiO catalyst particles; (b) several nucleation sites generated on one large ZnO grain; (c) continuous feeding of source elements into favorable nucleation sites of the ZnO grain leading to vertical growth of ZnO nanowires; (d) lateral growth of ZnO nanowires; (e) formation of the incomplete ZnO tubular structure; (f) perfect ZnO microtubes formed by the coalescence of neighboring nanowires.

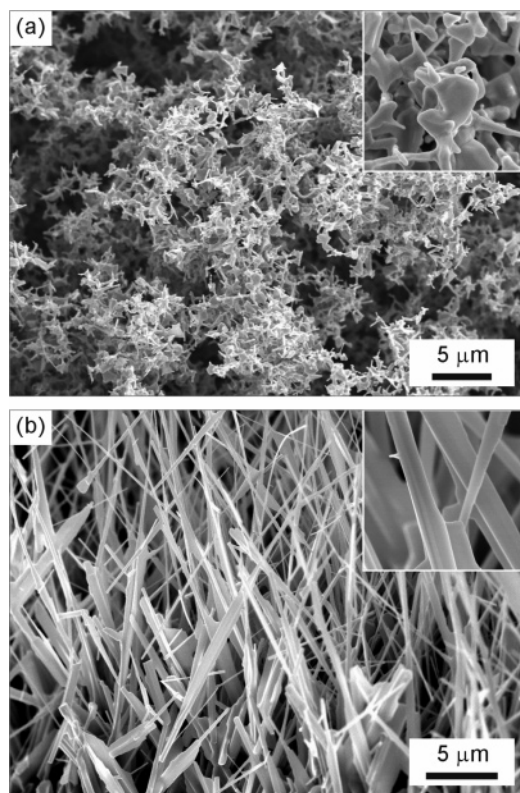


**Figure 7.** Typical SEM images of the ZnO crystals synthesized under oxygen flow of (a) 50 sccm and (b) 2 sccm with argon flow of 500 sccm at 950 °C.

condition.<sup>27,28</sup> This is consistent with the growth behavior of the ZnO microtubes synthesized by our experiment. It is well-known that the crystal facets with lower growth rate appear while the crystal facets with higher growth rate

disappear. Therefore, although the  $\{01\bar{1}1\}$  facets are not observed under our experimental condition, the  $\{01\bar{1}0\}$  facets appear in the synthesized ZnO microtubes as shown in the SEM images. It is suggested that the lateral growth of the ZnO nanowires which is accelerated by high reaction temperature induces the coalescence of the neighboring nanowires and the ZnO microtubes formed by the coalescence of the nanowires finally exhibit a stable hexagonal crystal shape with  $\{01\bar{1}0\}$  facets as shown in Figure 6f. This is the reason the incomplete ZnO microtubes stopped at different stage of their growth also have a crystal shape similar to the hexagonal shape in their morphology as shown in Figure 4.

## Conclusions

We demonstrated that the single-crystalline wurtzite ZnO microtubes were fabricated on NiO-catalyzed  $\text{Al}_2\text{O}_3$  substrate using a simple metal-vapor deposition method. The ZnO microtubes, which had outer diameters in the range of 0.3–2  $\mu\text{m}$  and wall thickness in the range of 100–500 nm, indicated a faceted hexagonal shape. In addition, it was found that there were many incomplete ZnO microtubes, which indicated the morphology assembled with several nanowires at the tip part of the microtubes and prismatic tubular morphology at the bottom part of the microtubes. It is suggested that the tubular structures are formed by the coalescence of ZnO nanowires grown on a large ZnO grain at a high reaction temperature of 950 °C under an oxygen ambient.

**Acknowledgment.** This work was supported by Grant No. R-11-2000-086-0000-0 from the Center of Excellence Program of the Korea Science and Engineering Foundation and Ministry of Science and Technology, National R&D Project for Nano Science and Technology of MOST, and Center for Nanotubes and Nanostructured Composites at Sungkyunkwan University.

CM049387L

(27) Li, W.-J.; Shi, E.-W.; Zhong, W.-Z.; Yin, Z.-W. *J. Cryst. Growth* **1999**, 203, 186.

(28) Laudise, R. A.; Ballman, A. A. *J. Phys. Chem.* **1960**, 64, 688.